Hydrology and Earth System Sciences

Open Access

Discussions

Investigation of hydrological time series using copulas for detecting catchment characteristics and anthropogenic impacts

T. Sugimoto[1], A. Bárdossy[1,2], G. S. S. Pegram[2], and J. Cullmann[3]

[1]Institute for Modelling Hydraulic and Environmental Systems, University of Stuttgart, Stuttgart, Germany
[2]Civil Engineering Program, University of KwaZulu-Natal, Durban, South Africa
[3]Federal Institute of Hydrology, Koblenz, Germany

Abstract

Global climate change can have impacts on characteristics of rainfall-runoff events and subsequently on the hydrological regime. Meanwhile, the catchment itself changes due to anthropogenic influences. In this context, it can be meaningful to detect the temporal changes of catchments independent from climate change by investigating existing long term discharge records. For this purpose, a new stochastic system based on copulas for time series analysis is introduced. While widely used time series models are based on linear combinations of correlations assuming a Gaussian behavior of variables, a statistical tool like copula has the advantage to scrutinize the dependence structure of the data in the uniform domain independent of the marginal.

Two measures in the copula domain are introduced herein:

1. Copula asymmetry is defined for copulas and calculated for discharges; this measure describes the non symmetric property of the dependence structure and differs from one catchment to another due to the intrinsic nature of both runoff and catchment.

2. Copula distance is defined as Cramér-von Mises type distance calculated between two copula densities of different time scales. This measure describes the variability and interdependency of dependence structures similar to variance and covariance, which can assist in identifying the catchment changes.

These measures are calculated for 100 years of daily discharges for the Rhine rivers. Comparing the results of copula asymmetry and copula distance between an API and simulated discharge time series by a hydrological model we can show the interesting signals of systematic modifications along the Rhine rivers in the last 30 years.

1 Introduction

In order to understand the water cycle behavior of a region, it is important to determine its characteristics, but this is difficult to achieve due to the diversity of the system response at different time and space scales. In particular, temporal variability makes parameter estimation difficult and the assessment of model uncertainty essential. As a part of the endeavor to grasp the hydrological system, the objective of this research, assessing the anthropogenic impacts on the catchment characteristic independent of the climate change is therefore important, yet hard to accomplish.

The first possible approach is to statistically test the existence or change of trend in hydrological time series which can be related to climate changes or anthropogenic impacts. Mann-Kendall's Test was performed to confirm the existence of a trend in the annual discharge, precipitation and sediment loads and discussed the human intervention and climate impacts based on the available information of the catchments (Wu et al., 2012). Pettitt's Method (Pettitt, 1979) can be used to detect the time point of trend alternation and analyze the impacts based on a double mass curve (Gao et al., 2013) or a hydrological model (Karlsson et al., 2014). These non-parametric methods for detecting the signal seem, however, not capable enough of explaining when and how much the system had changed, thus making it still difficult to relate the change to human activities.

On the other hand, runoff events are initiated by precipitation then modified by the state and physical features of the catchment. This implies that the integrated information of catchment status might be retrieved by analyzing the discharge time series itself. Focusing on this property, the attempts can be made for capturing the temporal dependence structure of runoff by time series models. The classical time series model, autoregressive integrated moving average (ARIMA), is designed to describe a stationary stochastic process based on the temporal correlation structure of Gaussian random variables (Box and Jenkins, 1976). However, the stationarity of the data is not guaranteed in reality, thus a number of alternative approaches have been suggested.

Empirical mode decomposition (Huang et al., 1998) is a method designed to overcome the drawbacks of Fourier analysis by allowing the frequency and local variance of a time series to vary within a component and to separate the signals adaptively by scale. Autoregressive Conditional Heteroskedasticity (ARCH) models loose the assumption of stationarity to a certain extent so that variance is not constant, however models the variance in a similar way to ARIMA. Although the inventions and efforts to overcome the limitation of stationarity are made, it seems still inadequate to model dynamic changes of hydrological processes with these time series models.

Alternatively there is a statistical concept, copulas, which has advantages to model the multivariate dependence independently from marginals and recently adopted in the field of hydrology. A Copula (Sklar, 1959) is a multivariate probability distribution designed to flexibly model dependence structure in the uniform (quantile) domain. The use of copulas in hydrology can be found for the assessment of extreme events by considering flooding as a joint behavior of peak and volume (De Michele and Salvadori, 2003). Copulas have been applied to describe the spatio-temporal uncertainty of precipitation (Bárdossy and Pegram, 2009) or the inhomogeneity of groundwater parameters (Bárdossy and Li, 2008). Asymmetry of dependence in a time series can be tested in the framework of a finite state Markov chain's transition probability matrix (Sharifdoost et al., 2009). Dissimilarity measures can be defined by means of a copula modelling the correlation structure of pairs of discharge time series in order to identify the similarity of catchments with the purpose of transferring catchment properties from one to the other (Samaniego et al., 2010). We aim at utilizing copulas as an alternative to classical time series models and an efficient tool for time series analysis to overcome these hydrological challenges.

The main interest of this study is to precisely assess the human intervention and climate change impacts on hydrological regime for the strategy of future development in the region. For achieving this goal, 7 daily discharge gauging stations in South-West Germany (Fig. 1), which have 100 years daily discharge records, were chosen and extensively analyzed. The gauging stations Andernach, Kaub, Worms and Maxau are

located in the main stream of the Rhine, while Kalkofen, Cochem and Plochingen are located on tributaries. For further analysis, daily precipitation and temperature records in the Baden-Württemberg state of Germany for the last 50 years were obtained from the German Weather Service. Also, 77 discharge records obtained from the Global Runoff Date Centre in Germany were utilized.

What follows is the new aspects introduced in this study: (1) The catchment characteristic is defined based on copulas and estimated from discharge data. Also the changes of catchment characteristic are investigated by tracing the temporal change of this statistics. (2) A method to model systematic changes of dependence structure with the help of copulas is suggested, then its variability and interrelationship of the time series are examined. (3) Anthropogenic impacts are assessed by the discharge – precipitation relation using API and hydrological model with copula based measures.

This article is divided into five sections. After the introduction, the basic methodology for applying copulas to discharge time series is introduced in the second section. Thirdly, the measures of asymmetry in copulas are defined and estimated for the discharges of the river Rhine and other catchments. The determination of the temporal change of the asymmetry of the copulas is treated in the third section as well. In the fourth section two topics are treated: (i) the analysis based on copula distances for the observed discharges and (ii) the comparison of observed discharge with API (Antecedent Precipitation Index) time series and simulated discharge time series with a hydrological model. The conclusion is given in the fifth section.

2 Methodology

In this section, the application of copula to time series is articulated after a brief introduction of copulas. The very basics about copulas are presented here and further information can be obtained from (Joe, 1997) or (Nelsen, 1999).

2.1 Basic methodology

In probability theory and statistics, a copula is a multivariate probability distribution for which the marginal probability distribution of each variable is uniform.

$$C : [0, 1]^n \rightarrow [0, 1] \tag{1}$$

$$C\left(\boldsymbol{u}^{(i)}\right) = u_i \ \ if \ u^{(i)} = (1, \ldots, 1, u_i, 1, \ldots 1). \tag{2}$$

Any multivariate distribution can be described by a copula and its marginal distributions as was proven by Sklar's theorem (Sklar, 1959):

$$F(\boldsymbol{x}) = C\left(F_{X_1}(x_1), \ldots, F_{X_n}(x_n)\right), \tag{3}$$

where $F_{X_i}(x_i)$ represents the i-th marginal distribution of a multivariate random variable $\boldsymbol{X}$. The copula density can be derived by taking partial derivatives of the copula:

$$c(u_1, \ldots, u_n) = \frac{\partial^n C(u_1, \ldots, u_n)}{\partial u_1 \ldots \partial u_n}. \tag{4}$$

The advantage of using copulas is that the marginal is detached from the multivariate distribution and the dependence structure can be examined in the uniform compact domain for different types of data.

2.2 Basic hypothesis of temporal copulas

For the application of copulas to time series analysis, a stochastic system should be presumed to be similar to the case of spatial copulas (Bárdossy and Li, 2008): the random variable at time t is described as $Z(t)$ and in general there may exist non-Gaussian dependency among the elements of $Z(t)$. Then stationarity is defined for each subset of times $t_1, \ldots, t_n \subset N$ and time lag k such that $\{t_1 + k \ldots, t_n + k\} \subset N$ and for each set of possible values $z_1, \ldots, z_n$:

$$P(Z(t_1) < z_1, \ldots, Z(t_n) < z_n) = P(Z(t_1 + k) < z_1, \ldots, Z(t_n + k) < z_n). \tag{5}$$

For the given random function $Z(t)$, a set $S(k)$ containing pairs of ranked values is defined as a function of time lag k as follows:

$$S(k) = \{(F_Z(z(t))), (F_Z(z(t+k)))\}. \tag{6}$$

Thus, a 2-dimentional autocopula for stochastic time series is a function of time lag k for the set $S(k)$ similar to the case of aspatial copula (Bárdossy and Li, 2008):

$$C_t(k, u_1, u_2) = P[F_z(Z(t)) < u_1, F_z(Z(t+k)) < u_2], \tag{7}$$

where $(u_1, u_2) \in S(k)$. Thus, a 2-dimentional empirical copula density can be constructed based on conditional empirical frequencies on a regular $g \times g$ grid and kernel density smoothing (Bárdossy, 2006):

$$c^* \left(\frac{2i-1}{2g}, \frac{2j-1}{2g} \right) = \frac{g^2}{|S(k)|} \cdot \left| \left\{ (u_1, u_2) \in S(k); \frac{i-1}{g} < u_1 < \frac{i}{g} \, and \frac{j-1}{g} < u_2 < \frac{j}{g} \right\} \right|, \tag{8}$$

where $|S(k)|$ denotes the cardinality (the number of elements in a set) of set $S(k)$.

3 Copula asymmetry in discharge time series

High and low values might have different dependences in general. Measuring the asymmetry of copulas could reveal substantial aspects of time series data, which are not illuminated in the Gaussian approach. Statistics defined on copula shape and calculated from observed discharge time series we believe to be a new idea. Asymmetry functions are defined on 2-dimensional copulas as a function of time lag k (Li, 2010). Asymmetry 1 is defined as:

$$A_1(k) = E\left[(U_t - 0.5)(U_{t+k} - 0.5)((U_t - 0.5) + (U_{t+k} - 0.5))\right]. \tag{9}$$

Asymmetry 2 is defined as:

$$A_2(k) = E\left[-(U_t - 0.5)(U_{t+k} - 0.5)((U_t - 0.5) - (U_{t+k} - 0.5))\right], \tag{10}$$

|◀ | ▶|

◀ | ▶

Back | Close

Full Screen / Esc

Printer-friendly Version

Interactive Discussion

where $u_t = F_Z(z(t)), u_{t+k} = F_Z(z(t+k))$. Figure 2 shows an idealization of the two asymmetries between a pair of variables $U(t)$ and $U(t+k)$, showing that the tails of the distributions have a large impact on each type of asymmetry. The measure of asymmetry (i) compares the dependency between low and high values and (ii) quantifies how much it is not symmetric. For example, in a 2-dimensional copula, $A_1(k)$ is positive if the probability density is higher in the upper right corner than in the lower left corner. On the other hand, $A_1(k)$ is negative if the probability density is higher in the lower left corner than in the upper right. $A_2(k)$ is the asymmetry for the other diagonal of a 2-dimensional copula. Figure 3 shows the scatterplot of ranked values of a discharge time series with time lag $k = 1$ as a sample of an empirical autocopula, demonstrating the structure is not symmetric especially for $A_2(k)$.

3.1 Asymmetry and catchment characteristics

Asymmetries can be considered as statistics calculated from the observed discharge time series and have an important assumption: "assymetry2 is related to catchment characteristics". This idea will be intensively discussed und demonstrated in this section. Figure 5 (upper left) shows part of the hydrographs of 7 gauging stations in southwest Germany.

First, an important and obvious natural property seen in this figure is that the duration of high flow and low flow periods is not symmetric: Flood events, which are initiated by rainfall or snowmelt, do not continue for a long time because the duration of runoff to rivers is comparatively short. On the other hand, discharge keeps decreasing and stays low for no rain periods. This means that, if two consecutive values in a time series are chosen for small time lag k, these two values are likely to be less correlated for high values but more correlated for low values, which leads to negative value to negative value of $A_1(k)$. This asymmetry can be related temporal distribution of precipitation.

Second, the increase and decrease of discharge is not symmetric: Soon after the rainfall, the river flow rises sharply. Once the rain stops and peak discharge is observed, then the water level starts to decrease, typically more slowly on the recession than the

rising limb of the hydrograph, which leads to negative values of $A_2(k)$ for small time lags k. This asymmetry can be related to the characteristics of the runoff and catchment.

The change of $A_2(k)$ with time lag k days is now discussed. The point is that these statistics for small time lags k can be more related to the catchment and rainfall characteristics of the region, while asymmetry for larger time lags k can capture the inter-seasonal characteristic of the climate in the region.

In order to reduce this seasonal impact, normalization was adopted for the time series similar to z-score in the following way. First, the annual cycle of the mean is calculated and smoothed by linear weighting

$$\mu_{t|365} = E\left[X_{t|365}\right] \tag{11}$$

$$\mu^*_{t|365} = \frac{1}{2N} \sum_{i=0}^{N/2} \left(\frac{1}{2} - \frac{i}{N}\right) \left(\mu_{t+i|365} + \mu_{t-i|365}\right), \tag{12}$$

where $t|365$ is $t\,(\mathrm{mod}\,365)$ and represents calendar day at time t [day]. X_i denotes the random variable of discharge, μ_i denotes mean and μ^*_i denotes mean after smoothing on calendar day i respectively. After subtraction of the annual mean from the original time series $Z(t)$, the annual cycle of standard deviation is defined.

$$\sigma_{t|365} = E\left[\sqrt{\left(X_{t|365} - \mu_{t|365}\right)^2}\right] \tag{13}$$

$$\sigma^*_{t|365} = \frac{1}{2N} \sum_{i=0}^{N/2} \left(\frac{1}{2} - \frac{i}{N}\right) \left(\sigma_{t+i|365} + \sigma_{t-i|365}\right). \tag{14}$$

Figure 4 shows the annual cycles after smoothing described by Eqs. (11) and (12). By subtracting the annual mean cycle and dividing by annual standard deviation cycle, the

normalized time series is defined.

$$Z_{norm}(t) = \left(\frac{Z(t) - \mu^*_{t|365}}{\sqrt{\sigma^*_{t|365}}} \right). \tag{15}$$

Figure 5 (upper right) shows part of normalized discharge time series from the 7 gauging stations. It should be noted that the process still appears to be non-Gaussian after this transformation and the seasonality for small time lags k might not be fully eliminated. Figure 5 (bottom left and bottom right) shows the variation of asymmetry functions for 7 discharge time series corresponding to time lag k similar to the correlograms in addition to the confidence interval of Gaussian process.

The confidence intervals in the figures are gained by calculating $A_2(k)$ for 100 realizations of stationary Gaussian process which are fitted to the observed discharge of Andernach. The result shows that the process is clearly different from Gaussian and the influence of asymmetry is significantly large.

It can be seen that the variation of $A_2(k)$ of discharge without normalization (Fig. 5 bottom left) has a larger impact of seasonality for bigger k ($k > 40$), while its impacts are mitigated after the normalization (Fig. 5 bottom right). Furthermore, as a consequence of normalization, a sharp drop down of $A_2(k)$ for small time lags k emerged which might be regarded as a catchment indicator. Therefore, the selected/critical properties for small time lags k is formulated by (i) taking the minimum value of $A_2(k)$ for the time lag $k < 50$ and (ii) the lag k at the minimum of asymmetry2:

$$A_{2,min} = \min_{k<50} A_2(k) \tag{16}$$

$$L_{2,min} = \min_{0<k<50} \{k; A_2(k) = A_{2,min}\}. \tag{17}$$

The question is whether they are really related to catchment characteristics. Now, these statistics estimated for 77 discharge data recorded at the gauging stations in Germany

are compared with the catchment area as one of the simplest possible indicators of the catchment as shown in Fig. 6: $A_{2,\min}$ – *area* (Fig. 6 top) shows a more clear linear relation than $L_{2,\min}$ – area (Fig. 6 middle) while the dispersions $A_{2,\min}$ and $L_{2,\min}$ for the smaller catchments are big for both cases. The correlation between $A_{2,\min}$ and $L_{2,\min}$ (Fig. 6 bottom) is slightly positive.

This demonstrates that the information extracted from discharge is related to the basic information of its catchment to a certain extent. Since the principal objective is to assess anthropogenic impacts, the idea introduced now is to use this measure for evaluating the catchment change by calculating chronological changes of $A_{2,\min}$.

3.2 Time series analysis with asymmetry

Temporal change of asymmetry $A_2(k,t)$ is defined on the set representing a moving time window of size w.

$$S^*(k,t) = \left\{ (F_Z(z(a))),(F_Z(z(a+k)));t - \tfrac{w}{2} < a < t + \tfrac{w}{2} \right\} \tag{18}$$

$$A_2(k,t) = E\left[(U_t - 0.5)(U_{t+k} - 0.5)((U_t - 0.5) + (U_{t+k} - 0.5))\right], \tag{19}$$

where $u_t \in U_t, u_{t+k} \in U_{t+k}, \left(u_t, u_{t+k}\right) \in S^*(k,t)$.Then the minimum of asymmetry2 and lag k at the minimum of asymmetry2 at time t are given by

$$A_{2,\min}(t) = \min_{k<30} A_2(k,t) \tag{20}$$

$$L_{2,\min}(t) = \min_{0<k<30} \left\{k; A_2(k,t) = A_{2,\min}(t)\right\}. \tag{21}$$

Figure 7 shows the temporal changes of $A_{2,\min}(t)$ with window size $w = 3000$ days for 7 gauging stations in southwest Germany in addition to the confidence interval calculated for 100 times independently generated Gaussian process.

The comparison of $A_{2,\min}(t)$ from observed discharges with $A_{2,\min}(t)$ from a Gaussian process exhibits (i) the influence of asymmetry in discharge is significantly large as it

was seen in Fig. 5. (ii) The fluctuations of $A_{2,\min}(t)$ of 7 observed discharge time series appear to be bigger than the one calculated for a realization of a Gaussian process. (iii) $A_{2,\min}(t)$ of these 7 discharge records shows a similar trend: there are big drop-downs around 1945 and after 1980 for all the discharges.

However, it cannot be ascertained whether this is caused by the simultaneous change of the catchments, the long term meteorological behavior in the region or just randomness in the stationary process. To overcome this, temporal behavior of discharge and temperature were first checked by calculating the mean, the standard deviation and the minimum at time t defined by

$$\text{Mean}(t) = \frac{1}{w} \int_{t-w/2}^{t+w/2} z(a)\,da$$

$$\text{Std}(t) = \sqrt{Var(t)} = \frac{1}{w}\left(\int_{t-w/2}^{t+w/2} (z(a) - E[Z(t)])^2 da \right)^{\frac{1}{2}}$$

$$\text{Min}(t) = \min\left\{ Z(a); t - \frac{w}{2} < a < t + \frac{w}{2} \right\}, \tag{22}$$

where w is the size of time window. Figure 8 shows moving average and moving standard deviation of discharge records with windows size $w = 3000$ days, but it is hard to say whether the behavior around 1945 and after 1980 is unusual. Figure 9 shows mean and minimum of temperature in the time window with size 365 days which correspond to annual mean and minimum. Roughly speaking, there are certain cold periods around 1940, 1955 and 1985, which might influence the snow accumulation and melting in the region, but the relation with asymmetry2 is rather obscure.

What seems to be a useful outcome from the above exploratory analysis is that (i) the behavior of asymmetry2 is different from catchment to catchment showing a statistical relation with the catchment area and (ii) temporal behaviors of asymmetry2

of 7 discharges time series are dependent on each other, which implies the existence of a background mechanism common to the region.

4 Analysis of hydrological time series with Copula Distance

As an alternative to copula asymmetry, which emphasizes the behavior on the corner of copulas, copula distance is here suggested so that the characteristic behavior can be captured in the entire domain of the copula. Calculating this for each time step for different time series and comparing them hopefully exhibits the changes of dependence structure and therefore the catchment change.

4.1 Introduction of Copula Distance

The basic idea behind the copula distance is to apply the Cramér-von Mises type distance

$$D = \int_0^1 \int_0^1 (C^*(u_1, u_2) - C(u_1, u_2))^2 \, du_1 \, du_2, \qquad (23)$$

which by design measures the goodness of fit between two distribution functions, to two copulas. This type of distance was tested to measure the difference between empirical and theoretical copula in the bootstrap framework for the evaluation of spatial dependence of ground water quality (Bárdossy, 2006). For the analysis of time series data, it still needs to be carefully thought out how (and which) copulas should be chosen.

4.1.1 Introduction of Copula Distance to single time series

In order to apply the concept of copula distance to time series, the adoption of two copulas in different time scales is considered. An empirical copula can be obtained from an entire time series which contains the averaged information of all the time points

(*global copula*). Another empirical copula can be obtained for a certain window of width w at time step t (*local copula*). In order to make the concept clear, two sets containing pairs of ranked values with different time scales are specified.

$$S_{\text{global}}(k) = \{(F_Z(z(t))),(F_Z(z(t+k)));t_1 < t < t_n\} \tag{24}$$

$$S_{\text{local}}(k,t) = \left\{ \begin{array}{c} (F_Z(z(a))),(F_Z(z(a+k))) \\ ;t - \frac{w}{2} < a < t + \frac{w}{2} \end{array} \right\}. \tag{25}$$

$S_{\text{local}}(k,t)$ can be interpreted as a moving time window where the reference time t is set to the middle of the window of size w, while $S_{\text{global}}(k)$ represents a set of the entire time series. *Global copula* and *local copula* are the empirical autocopula densities defined on these sets based on Eq.(8), there denoted by $c^*_{\text{global}}(\boldsymbol{u})$ and $c^*_{\text{local}}(\boldsymbol{u},t,w)$ respectively for the n-dimensional case. In this analysis, 3000 days for the time window w and a 3-dimensional copula separated with 1 day gap between each variable are employed. This means

$$\boldsymbol{u} = (u_0,u_1,u_2), \tag{26}$$

where $u_0 = F_z(Z(t)), u_1 = F_z(Z(t+1)), u_2 = F_z(Z(t+2))$, then the deviation of local copula from global copula is defined by

$$\Delta c(\boldsymbol{u},t) = c^*_{\text{local}}(\boldsymbol{u},t) - c^*_{\text{global}}(\boldsymbol{u}). \tag{27}$$

For the first approach, the comparison of dependence structures between entire and local time series is done for detecting unusual dependence structures. To this end, *copula distance type1* is defined by taking the copula distance between global and local copula at each time step t

$$D_1(c,t) = \int_0^1 \cdots \int_0^1 \left(c^*_{\text{global}}(\boldsymbol{u}) - c^*_{\text{local}}(\boldsymbol{u},t) \right)^2 du_1 \ldots du_n = \int_0^1 \cdots \int_0^1 \Delta c(\boldsymbol{u},t)^2 du_1 \ldots du_n. \tag{28}$$

Second, *copula distance type 2* is introduced for indicating the point at which the structure of copulas starts to change. For this method, the distance between two local copulas is calculated from the 2 time intervals

$$D_2(c,t) = \int_0^1 \cdots \int_0^1 \left(c^*_{\text{local}}\left(\boldsymbol{u}, t - \frac{w}{2}\right) - c^*_{\text{local}}\left(\boldsymbol{u}, t + \frac{w}{2}\right) \right)^2 du_1 \ldots du_n. \tag{29}$$

Note that reference time is set to the middle of both time windows and shifted for *w/2* days from each other where the size of the time windows is *w*. Therefore, there is no overlapping part between the two time intervals of these two local copulas. For the comparison, the moving variance is introduced as follows:

$$E\left[Z(t)\right] = \frac{1}{w} \int_{t-w/2}^{t+w/2} z(a)\,da \tag{30}$$

$$\text{Var}(t) = \frac{1}{w} \int_{t-w/2}^{t+w/2} (z(a) - E\left[Z(t)\right])^2 da. \tag{31}$$

Figure 10 shows the result of $D_1(t)$, $D_2(t)$ and $\text{Var}(t)$ in the moving time window for the normalized discharge time series between 1940 to 2000 at 4 gauging stations located in the main stream of the Rhine (Andernach, Maxau) and its two different tributaries (Cochem, Plochingen) in addition to the 90 % confidence intervals calculated for the Gaussian process fitted to the discharge data of Andernach.

First of all, the values of these 2 measures at Cochem and Plochingen are bigger and more fluctuating in general. The reason could be that their catchments and discharges are smaller, thus more sensitive to changes. Second, it can be said that the dependence structure is not homogeneous over the time period, but the local copula clearly deviates from the global copula for certain time periods. For example, the value

of $D_1(t)$ is remarkably big around 1947, 1982 and 2000 for all the 4 discharge records (pointed by white arrows). $D_2(t)$ is also big around 1977 for all the data. This signal of $D_2(t)$ implies that a simultaneous change of runoff behavior occurred in this region at 1977, which can be related to the high value of $D_1(t)$ at 1982. Var(t) is also changing, but the direct relation with $D_1(t)$ and $D_2(t)$ is hard to recognize. Also the confidence interval of the Gaussian process is clearly smaller than the observed one. This indicates the copula distances of the stationary process are small while the nature process is non-stationary and its dependence structure is more varying.

For copula distance type1, the global copula can be considered as an average state of the copula, while the local copula can be regarded as a realization of a possible state of a copula at time step t. This concept can be comparable to variance and leads to a new measure, *copula variance*, which is the summation of copula distances between global and local copula over the time.

$$\text{Var}_{\text{cop}}(c) = \frac{1}{t_n - t_1} \int_{t_1}^{t_n} D_1(c,t)\,dt. \tag{32}$$

Table 1 shows the variance and copula variance calculated for the 4 discharge data. The result demonstrates that copula variance of the time series can be higher, even if the conventional variance is lower for example in case of Maxau.

4.1.2 Copula Distance for two time series

In the previous section, copula variance was defined as a measure of the variability characteristic of the copula itself. Here, it is examined whether covariance can be defined for two copula densities c_1 and c_2 from two time series as *copula distance type3*,

Title Page

Abstract | Introduction

Conclusions | References

Tables | Figures

|◀ | ▶|

◀ | ▶

Back | Close

Full Screen / Esc

Printer-friendly Version

Interactive Discussion

which shows whether the variability characteristic of copulas is related to each other.

$$D_3(c_1, c_2, t) = \int_0^1 \ldots \int_0^1 \Delta c_1(\boldsymbol{u}, t) \Delta c_2(\boldsymbol{u}, t) \, du_1 \ldots du_n, \tag{33}$$

where

$$\begin{cases} \Delta c_1(\boldsymbol{u}, t) = c_{1,\text{local}}^*(\boldsymbol{u}, t) - c_{1,\text{global}}^*(\boldsymbol{u}) \\ \Delta c_2(\boldsymbol{u}, t) = c_{2,\text{local}}^*(\boldsymbol{u}, t) - c_{2,\text{global}}^*(\boldsymbol{u}) \end{cases}. \tag{34}$$

5 By its definition, the value of $D_3(t)$ can be related to $D_1(t)$ because $D_3(t)$ compares the deviation of local copulas from global copulas in a similar way to $D_1(t)$ in Eq. 28. In order to reduce the influence of $D_1(t)$ on $D_3(t)$, *copula distance type4* is introduced as a normalized measure bounded between -1 and 1 analogous to correlation.

$$D_4(c_1, c_2, t) = \frac{D_3(c_1, c_2, t)}{\sqrt{D_1(c_1, t)} \cdot \sqrt{D_1(c_2, t)}}, \tag{35}$$

10 where $|D_4(c_1, c_2, t)| \leq 1$. For comparison, covariance and correlation in a moving window are introduced for two random variables $Z_1(t)$ and $Z_2(t)$ as follows:

$$\text{Cov}(t) = \int_{t-w/2}^{t+w/2} (z_1(a) - E[Z_1(t)])(z_2(a) - E[Z_2(t)]) \, da \tag{36}$$

$$\text{Cov}(t) = \frac{\text{Cov}(t)}{\sqrt{\text{Var}(Z_1(t))} \cdot \sqrt{\text{Var}(Z_2(t))}}. \tag{37}$$

Figure 11 shows the copula distance between two time series $D_3(t)$ and $D_4(t)$ in addition to the covariance and correlation in moving time window.

Title Page

Abstract | Introduction

Conclusions | References

Tables | Figures

◀ | ▶|

◀ | ▶

Back | Close

Full Screen / Esc

Printer-friendly Version

Interactive Discussion

Full Screen / Esc

Printer-friendly Version

Interactive Discussion

First, it can be said that the behavior of covariance and correlation in a moving window are different from $D_3(t)$ and $D_4(t)$. This implies these two copula based statistics exhibit different properties of the time series from ordinary statistics. Second, $D_3(t)$ shows high values around around 1947, 1982 and 2000, which is same to the case of $D_1(t)$ in Fig. 10. This indicates that unusual states of copulas in 4 discharge time series can be related to each other. Third, $D_4(t)$ is in general high except for the period around 1970 and 1990. This means, the temporal behavior of dependence structures for these 4 discharges are actually similar except for these periods even if $D_1(t)$ and $D_3(t)$ are small.

Copula covariance and copula correlation can be defined similar to copula variance in order to quantify the overall behavior of two time series.

$$\mathrm{Cov}_{\mathrm{cop}}(c_1, c_2) = \frac{1}{t_2 - t_1} \int_{t_2}^{t_1} D_3(t)\, \mathrm{d}t \tag{38}$$

$$\mathrm{Cor}_{\mathrm{cop}}(c_1, c_2) = \frac{\mathrm{Cov}_{\mathrm{cop}}(c_1, c_2)}{\sqrt{\mathrm{Var}_{\mathrm{cop}}(c_1)} \cdot \sqrt{\mathrm{Var}_{\mathrm{cop}}(c_2)}}, \tag{39}$$

where $\left| \mathrm{Cor}_{\mathrm{cop}}(c_1, c_2) \right| \leq 1$ and its derivation can be found in Appendix A. In Table 2, these copula based statistics are compared with ordinary statistics. For example, Cochem and Plochingen are located remotely in different tributaries, thus covariance and correlation are lower than the others, but copula covariance and copula correlation are not the lowest.

The measures using copula distance are different from the conventional statistics. This behavior can be explained by the fact that the autocopula has more substantial information about temporal dependence structure than the autocorrelation. Using these measures might enable us to take advantage of a different way of seeing the dependence between time series.

What is new in the analysis of this section is that (i) measures based on copula distance show the different properties of time series in comparison to conventional statistics and (ii) there are significant signals of copula distances for certain time periods in common to all the discharge data.

4.2 Copula based stochastic analysis with API and hydrological model

The difficulty of analyzing discharge time series in order to detect catchment change is that it is not clear whether the temporal change of stochastic information is caused by catchment change or merely by random behavior of precipitation. To gain an understanding of this process, we attempted to eliminate the influence of precipitation using, first, API (antecedent precipitation index) for comparison with discharge, second, using a hydrological model with the parameter sets calibrated and fixed for the entire simulation time period.

4.2.1 Copula Distance analysis with API

An API (Antecedent Precipitation Index) time series, which is generated from observed precipitation time series and behaves similarly to discharge, is used instead of precipitation.

$$\text{API}(t+1) = \alpha \text{API}(t) + P(t+1), \tag{40}$$

where $P(t)$ is daily precipitation [mm day^{-1}], API(t) is time series of API [mm day^{-1}] and $\alpha = 0.85$ was chosen. The assumption for this method is that the API time series has the stochastic information purely originated from the precipitation, while observed discharge is supposed to be influenced by both catchments and precipitations. If the stochastic information derived from these two data sets is the same, this indicates that the stochastic turbulence is originating from precipitation; otherwise the change is from the catchment.

For this investigation, precipitation data was carefully chosen for 4 regions (northwest, northeast, southwest and central) of Baden-Württemberg (Germany) so that they have several almost continuous daily records between 1935 and 2005. Figure 12 shows the locations of measuring stations. The precipitation time series were aggregated into one for each region by taking daily average, then 4 API time series was calculated in total by Eq. (40). Figure 13 shows the result of copula distances $D_1(t)$, $D_2(t)$ and moving average Var(t) for API time series with the 90 % confidence intervals of the Gaussian process. Figure 14 shows the result of copula distances $D_3(t)$, $D_4(t)$ and moving covariance and correlation for API time series.

What can be recognized first in this Fig. 13 is that the magnitudes of $D_1(t)$ and $D_2(t)$ are smaller than the case of discharge. This is considered to happen as a result of aggregation of precipitation time series and adoption of API, but some signals can be still identified: $D_1(t)$ around 1947 and 2000 is high, but not much for 1982. The signal of $D_2(t)$ which was detected around 1977 in Fig. 11 does not seem to exist for API. This can be even more clear for $D_3(t)$ in Fig. 14 that there is no common change of the dependence structure around 1982 in API time series. This is interesting due to the following implications: (i) the noises of $D_1(t)$ in Fig. 13 were reduced and signals in common were amplified (ii) the unusual state of copula around 1982 is not caused not by precipitation, but could be caused by the catchment change.

For further verification, copula distance type3 and type4 between discharge and API time series were calculated as shown in Fig. 15. This result also shows there is no clear relation between API and discharge time series around 1982.

4.2.2 Copula based analysis with a hydrological model

API time series were calculated by spatially aggregating several daily precipitations records in each region of Baden-Württemberg state. In this section, simulated discharges time series are generated by a conceptual hydrological model, HBV (Bergström 1976; Bergström et al., 1995), which takes daily precipitations and temperatures records as input and simulates discharges for smaller catchments as more

robust sample of discharge to compare with observed discharge in order to check if differences might occur due to the method.

Thus the idea behind this methodology is similar to the case of API: A hydrological model with the parameters fixed for the entire time period represents the catchment not influenced by anthropogenic impacts. Then, the discharges simulated by this model should not reflect on the catchment change, while observed discharge is assumed to be influenced by both catchment and precipitation.

For the study area, upper Neckar catchment was chosen as drawn in Fig. 12. One parameter set needed for this model constitutes of 13 parameters which are calibrated based on the Nash–Sutcliffe model efficiency coefficient using the simulated annealing algorithm for the period between 1960 and 2000. Then, 30 parameter sets are independently calibrated in total and, subsequently, 30 simulated discharges time series are generated to compare with one observed discharge.

Figure 16 shows the result of copula based analysis calculated for single time series $(D_1(t), D_2(t), A_{2,\min}(t))$. It can be seen that $A_{2,\min}(t)$ in Fig. 16 (top) that (i) fluctuations of $A_{2,\min}(t)$ of observed and simulated discharge are locally identical. This implies that the short term behavior of $A_{2,\min}(t)$ is originated from the temporal behavior of precipitation but (ii) there exists a change of trend around 1976: $A_{2,\min}(t)$ of observed discharge is slightly bigger than simulated before 1976, while $A_{2,\min}(t)$ of observed discharge clearly undershoot the simulated ones of after 1976. This change of trend was also seen in the previous analyses ($D_2(t)$ in Fig. 10). Furthermore, $D_1(t)$ in Fig. 16 (middle) is high before 1976 which indicates the state of the copula is different from the rest, while the result of simulated discharges does not show such tendency. $D_2(t)$ in Fig. 16 (bottom) indicates the change of dependence structure happened around 1970 and 1977. These results using the HBV model indicate the change of the dependence structure detected using copulas around 1976 is not caused by the random behavior of precipitation, but by the behavior of the catchment itself.

The fact and the notion obtained in this section is that (i) both results from API and HBV based on copula measures indicate that the catchment changed around 1976 and

(ii), by comparing the simulated discharge with observed discharge, the origin of the change of stochastically information can be assessed.

5 Conclusion

In this paper the application of copulas for hydrological time series data is newly explored for the detection of catchment characteristics and their temporal changes.

1. A Copula based measure, asymmetry, was defined and newly applied for the identification of catchment characteristics. Indeed, it is presented that asymmetry2 can be related to the runoff characteristics.

2. The relation between the minimum of asymmetry2 and catchment characteristics was tested for 77 discharge records. Asymmetry2 has a certain relation especially with bigger catchments and this strengthens the notion that asymmetry2 can be used as a statistic to explain the catchment state.

3. Temporal change of asymmetry2 was calculated as an index of the catchment state and demonstrated it keeps changing with time. However, it is difficult to explain the causality, at least, by long term behavior of discharge and temperature time series.

4. A method based on copula distance was examined for the investigation of temporal behavior of hydrological time series. This measure can detect the time period where dependence structure is unusual and its interdependency. Clear signals were detected that the dependence structure is unusual for a certain time period and the signal was not found by investigating the time series with variance, covariance or correlation.

5. API time series were generated for each region in the Baden-Württemberg state and simulated discharge time series were generated using the HBV model for

Full Screen / Esc

Printer-friendly Version

Interactive Discussion

the upper Neckar catchment. These are the data not influenced by the catchment change, thus compared with observed discharge to assess the anthropogenic impacts. The results showed that there was a signal detected only in the observed discharge around 1982, but not in the API or simulated time series, which implies the anthropogenic impacts on the catchment. Also it was shown in the results of copula asymmetry that the difference of $A_{2,\text{min}}(t)$ between observed and simulated discharge was not constant, but the trend clearly changed around 1976.

The results of copula based analysis of hydrological time series support the assumption that the catchment had started to change around 1976 and stayed unusual until 1990. These changes could correspond to the construction of flood retention basins started around 1982 (Lammersen et al., 2002) and ecological flooding strategy, which let small floods to happen for the rehabilitation of ecological systems in the floodplain, introduced in the Upper Rhine since 1989 (Siepe, 2006).

Copulas can be an alternative method to analyze the hydrological time series data by focusing on the dependence structure. Empirical autocopula is a more data driven approach which retains more information than the copulas estimated with parametric methods, but it is also numerically demanding. The effective way to analyze time series and build up a time series model based on copula can be further explored.

Appendix A:

Suppose that a random variable at time t is denoted as $X(t)$ and $c_X(\boldsymbol{u}, t)$ is an autocopula obtained from $X(t)$. Assuming $c_{X,\text{mean}}(\boldsymbol{u})$ as an average state of $c_X(\boldsymbol{u}, t)$, deviation of copula $\Delta c_X(\boldsymbol{u}, t)$ at time t is defined by

$$\Delta c_X(\boldsymbol{u}, t) = c_X(\boldsymbol{u}, t) - c_{X,\text{mean}}(\boldsymbol{u}). \tag{A1}$$

For the empirical case, $c_X(\boldsymbol{u}, t)$ and $c_{X,\text{mean}}(\boldsymbol{u})$ can be regarded as local copula and global copula respectively similar to Eq. (31). Since global and local copula are empirical copula density as defined in Eq. (8), $\Delta c_X(\boldsymbol{u}, t)$ can be regarded as a vector of

values on finite number of grids:

$$\Delta \boldsymbol{c}_X(t) = \left(\Delta c_{X,1}(t), \Delta c_{X,2}(t), \ldots, \Delta c_{X,i}(t), \ldots, \Delta c_{X,N}(t) \right), \tag{A2}$$

where $\Delta c_{X,i}(t)$ denotes the value of copula density at i–th grid and N is the number of grids. From Cauchy-Schwarz inequality

$$\|\boldsymbol{\Delta} \boldsymbol{c}_X(t)\| \|\boldsymbol{\Delta} \boldsymbol{c}_Y(t)\| \geq |\langle \boldsymbol{\Delta} \boldsymbol{c}_X(t), \boldsymbol{\Delta} \boldsymbol{c}_Y(t) \rangle|^2, \tag{A3}$$

where $\|\boldsymbol{\Delta} \boldsymbol{c}_X(t)\|$ is L^2-norm and $\langle \boldsymbol{\Delta} \boldsymbol{c}_X(t), \boldsymbol{\Delta} \boldsymbol{c}_Y(t) \rangle$ is inner product of vector $\boldsymbol{\Delta} \boldsymbol{c}_X(t)$ and $\boldsymbol{\Delta} \boldsymbol{c}_Y(t)$. Then

$$\|\boldsymbol{\Delta} \boldsymbol{c}_X(t)\| = \sum_{i=1}^{N} \Delta c_{X,i}(t)^2 = \int_0^1 \cdots \int_0^1 \Delta c_X(\boldsymbol{u}, t)^2 du_1 \ldots du_n = D_1(c_X, t) \tag{A4}$$

$$|\langle \boldsymbol{\Delta} \boldsymbol{c}_X(t), \boldsymbol{\Delta} \boldsymbol{c}_Y(t) \rangle|^2 = \langle \boldsymbol{\Delta} \boldsymbol{c}_X(t), \boldsymbol{\Delta} \boldsymbol{c}_Y(t) \rangle = \sum_{i=1}^{N} \Delta c_{X,i}(t) \cdot \Delta c_{Y,i}(t)$$

$$= \int_0^1 \cdots \int_0^1 \Delta c_X(\boldsymbol{u}, t) \Delta c_Y(\boldsymbol{u}, t) du_1 \ldots du_n = D_3(c_X, c_Y, t) \tag{A5}$$

$$\frac{|\langle \boldsymbol{\Delta} \boldsymbol{c}_X(t), \boldsymbol{\Delta} \boldsymbol{c}_Y(t) \rangle|^2}{\|\boldsymbol{\Delta} \boldsymbol{c}_X(t)\| \|\boldsymbol{\Delta} \boldsymbol{c}_Y(t)\|} = \frac{D_3(c_X, c_Y, t)^2}{D_1(c_X, t) \cdot D_1(c_Y, t)} = D_4(c_X, c_Y, t)^2 \leq 1. \tag{A6}$$

Therefore $|D_4(c_X, c_Y, t)| \leq 1$ in Eq. (32). Above inequality is valid for certain time point t and summing up Eq. (A6) for all the time steps t leads to

$$\sum_{t=1}^{T} \left(\|\boldsymbol{\Delta} \boldsymbol{c}_X(t)\| \cdot \|\boldsymbol{\Delta} \boldsymbol{c}_Y(t)\| \right) \geq \sum_{t=1}^{T} |\langle \boldsymbol{\Delta} \boldsymbol{c}_X(t), \boldsymbol{\Delta} \boldsymbol{c}_Y(t) \rangle|^2, \tag{A7}$$

where T is the number of time steps. $\|\Delta c_X(t)\|$ is a norm and can be denoted for simplicity as $x_t = \|\Delta c_X(t)\|$. Then

$$\sum_{t=1}^{T} \left(\|\Delta c_X(t)\| \cdot \|\Delta c_Y(t)\| \right) = \langle x, y \rangle, \tag{A8}$$

where $x = (x_1, x_2, \ldots x_T), y = (y_1, y_2, \ldots y_T)$ for $t = 1 \ldots T$. Again from Cauchy-Schwarz inequality

$$|\langle x, y \rangle|^2 \leq \|x\| \cdot \|y\|, \tag{A9}$$

where

$$\|x\| \cdot \|y\| = \sum_{t=1}^{T} x_t^2 \cdot \sum_{t=1}^{T} y_t^2 = \sum_{t=1}^{T} \|\Delta c_X(t)\|^2 \cdot \sum_{t=1}^{T} \|\Delta c_Y(t)\|^2$$

$$= \sum_{t=1}^{T} D_1(c_X, t)^2 \cdot \sum_{t=1}^{T} D_1(c_Y, t)^2 = T^2 \cdot \text{Var}_{\text{cop}}(c_X) \cdot \text{Var}_{\text{cop}}(c_Y) \tag{A10}$$

$$\langle x, y \rangle = \sum_{t=1}^{T} (x_t \cdot y_t) = \sum_{t=1}^{T} \left(\|\Delta c_X(t)\| \cdot \|\Delta c_Y(t)\| \right) \geq \sum_{t=1}^{T} |\langle \Delta c_X(t), \Delta c_Y(t) \rangle|^2$$

$$= \sum_{t=1}^{T} D_{3,XY}(t) = T \cdot \text{Cov}_{\text{cop}}(c_X, c_Y). \tag{A11}$$

Then $|\langle x, y \rangle|^2 \leq \|x\| \cdot \|y\|$ indicates

$$\left| \text{Cov}_{\text{cop}}(c_X, c_Y) \right|^2 \leq \text{Var}_{\text{cop}}(c_X) \cdot \text{Var}_{\text{cop}}(c_Y) \tag{A12}$$

$$\left| \text{Cor}_{\text{cop}} \right| = \frac{\text{Cov}_{\text{cop}}(c_X, c_Y)}{\sqrt{\text{Var}_{\text{cop}}(c_X)} \cdot \sqrt{\text{Var}_{\text{cop}}(c_Y)}} \leq 1. \tag{A13}$$

References

Bárdossy, A.: Copula-based geostatistical models for groundwater quality parameters, Water Resour. Res., 42, W11416, doi:10.1029/2005WR004754, 2006.

Bárdossy, A. and Li, J.: Geostatistical interpolation using copulas, Water Resour. Res., 44, W07412, doi:10.1029/2007WR006115, 2008.

Bárdossy, A. and Pegram, G. G. S.: Copula based multisite model for daily precipitation simulation, Hydrol. Earth Syst. Sci., 13, 2299–2314, doi:10.5194/hess-13-2299-2009, 2009.

Bergrström, S.: Development and application of a conceptual runoff model for Scandinavian catchments, Bulletin Series A, A]: [Bulletin series. Department of Water Resources Engineering, Lund Institute of Technology, University of Lund, 1976.

Bergstrom, S.: The HBV Model, edited by: Singh, V. P., Comput. Model. Watershed Hydrol., 443–476, 1995.

Box, G. E. P. and Jenkins, G. M.: Time series analysis, control, and forecasting, revised ed., Holden-Day, San Francisco, USA, 1976.

De Michele, C. and Salvadori, G.: A Generalized Pareto intensity-duration model of storm rainfall exploiting 2-Copulas, J. Geophys. Res. Atmos., 108, 4067, 2003.

Gao, P., Geissen, V., Ritsema, C. J., Mu, X.-M., and Wang, F.: Impact of climate change and anthropogenic activities on stream flow and sediment discharge in the Wei River basin, China, Hydrol. Earth Syst. Sci., 17, 961–972, doi:10.5194/hess-17-961-2013, 2013.

Huang, N. E., Shen, Z., Long, S. R., Wu, M. C., Shih, H. H., Zheng, Q., Yen, N.-C., Tung, C. C., and Liu, H. H.: The empirical mode decomposition and the Hilbert spectrum for nonlinear and non-stationary time series analysis, Proc. R. Soc. Ldn. Ser. A Math. Phys. Eng. Sci. 454, 903–995, 1998.

Joe, H.: Multivariate models and multivariate dependence concepts, Chapman & Hall, London, 1997.

Karlsson, I. B., Sonnenborg, T. O., Jensen, K. H., and Refsgaard, J. C.: Historical trends in precipitation and stream discharge at the Skjern River catchment, Denmark, Hydrol. Earth Syst. Sci., 18, 595–610, doi:10.5194/hess-18-595-2014, 2014.

Lammersen, R., Engel, H., Van de Langemheen, W., and Buiteveld, H.: Impact of river training and retention measures on flood peaks along the Rhine, J. Hydrol., 267, 115–124, doi:10.1016/S0022-1694(02)00144-0, 2002.

Li, J.: Application of copulas as a new geostatistical tool, Ph.D. Thesis, no.187, University of Stuttgart,Germany, 2010.

Nelsen, R. B.: An introduction to copulas, Springer, New York, doi:10.1007/0-387-28678-0, 1999.

Pettitt, A. N.: A non-parametric approach to the change-point problem, Appl. Stat., 126–135, 1979.

Samaniego, L., Bárdossy, A., and Kumar, R.: Streamflow prediction in ungauged catchments using copula-based dissimilarity measures, Water Resour. Res., 46, W02506, doi:10.1029/2008WR007695, 2010.

Sharifdoost, M., Mahmoodi, S., and Pasha, E.: A statistical test for time reversibility of stationary finite state Markov chains, Appl. Math. Sci., 52, 2563–2574, 2009.

Siepe, A.: Dynamische Überflutungen am Oberrhein?: Entwicklungs-Motor für die Auwald-Fauna, Stand, 149–158, 2006..

Sklar, A.: Fonctions de répartition à n dimensions et leurs marges, Publications de l'Institut de statistique de l'Université de Paris, Publications de l'Institut de Statistique de L'Université de Paris, 8, 1959.

Singh, S. K., McMillan, H., and Bárdossy, A.: Use of the data depth function to differentiate between case of interpolation and extrapolation in hydrological model prediction, J. Hydrol., 477, 213–228, doi:10.1016/j.jhydrol.2012.11.034, 2013.

Sugimoto, T.: Copula based stochastic analysis of discharge time series. Ph.D. Thesis, no. 232, University of Stuttgart, Germany, 2014.

Wu, C. S., Yang, S. L., and Lei, Y. P.: Quantifying the anthropogenic and climatic impacts on water discharge and sediment load in the Pearl River (Zhujiang), China (1954–2009), J. Hydrol., 452–453, 190–204, doi:10.1016/j.jhydrol.2012.05.064, 2012.

Table 1. Variance and copula variance calculated for 4 discharge time series.

	ANDE	COCH	MAXA	PLOC
Var	1.79	2.24	1.75	2.72
Var_{cop} [$\times 10^{-5}$]	3.01	1.64	5.39	1.27

Table 2. Covariance, correlation, copula covariance and copula correlation between 4 discharge data (AN:Andernach, CO:Cochem, MA:Maxau, PL:Plochingen).

	AN-CO	AN-MA	AN-PL	CO-MA	CO-PL	MA-PL
Cov	1.68	1.60	1.33	1.38	1.31	1.41
Cor	0.84	0.90	0.60	0.70	0.53	0.64
Cov_{cop} [$\times 10^{-6}$]	4.90	3.40	3.39	7.16	9.90	5.47
Cor_{cop}	0.60	0.77	0.46	0.71	0.60	0.59

Full Screen / Esc

Printer-friendly Version

Interactive Discussion

Table 3. Variance and copula variance calculated for API time series of 4 regions in the Baden-Württemberg state of Germany.

	C	SW	NW	NE
Var	1.70	1.66	1.72	1.78
Var_{cop} [$\times 10^{-6}$]	3.00	4.02	3.35	3.21

Table 4. Covariance, correlation, copula covariance and copula correlation between API time series from 4 regions in the Baden-Württemberg state of Germany.

	C-SW	C-NW	C-NE	SW-NW	SW-NE	NW-NE
Cov	1.35	1.33	1.44	1.25	1.41	1.42
Cor	0.80	0.77	0.84	0.74	0.84	0.83
Cov_{cop} $[\times 10^{-7}]$	1.46	1.16	8.94	4.42	1.11	8.80
Cor_{cop}	0.36	0.29	0.29	0.09	0.26	0.24

1) Andernach
2) Kaub
3) Worms
4) Maxau
5) Cochem
6) Plochingen
7) Kalkofen

N

0 20 40   80   120   160
Kilometers
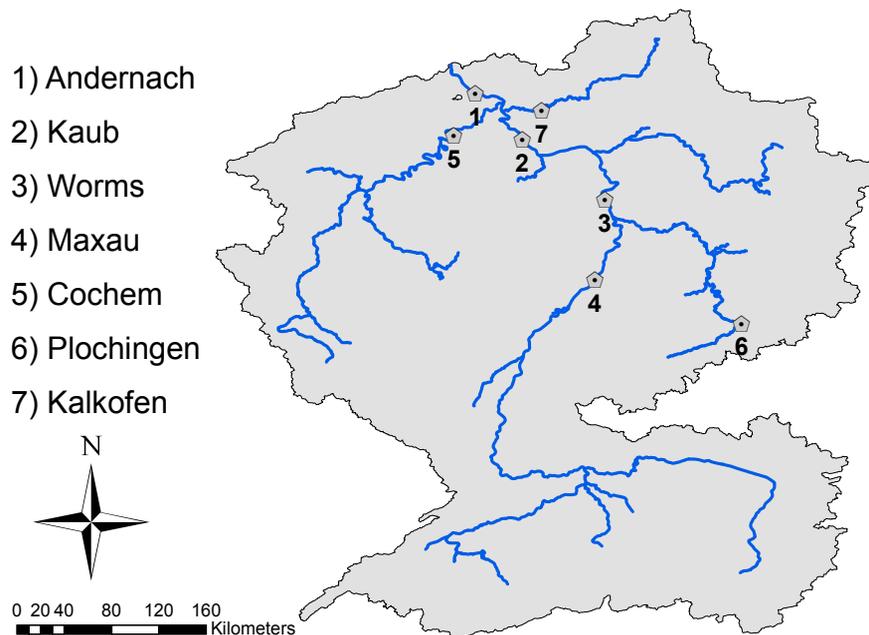
Figure 1. Locations of 7 discharge gauging stations in the Upper Rhine Region.

Figure 2. Visualization of the functions which displays the contribution of a realization of (U_t, U_{t+k}) to *asymmetry1* (left) and *asymmetry2* (right).
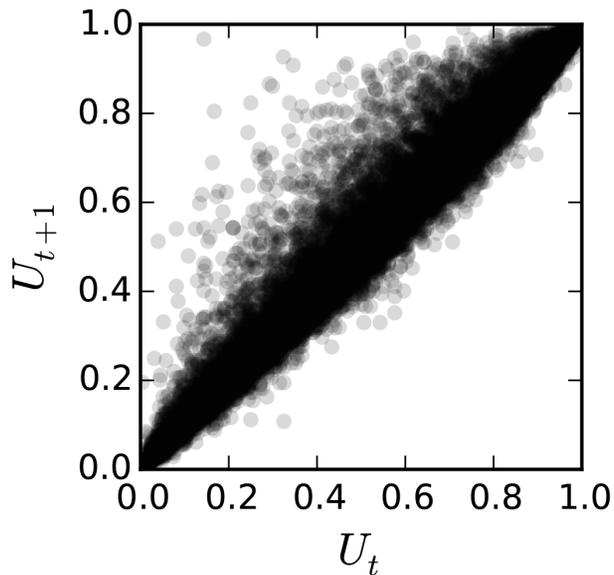
Figure 3. Scatterplot of ranks calculated from two values separated by time lag $k = 1$ [days] in a discharge time series of Andernach where rank correlation = 0.9870, $A_1(k = 1) = -0.0002398$ and $A_2(k = 1) = -0.00011037$.

Full Screen / Esc

Printer-friendly Version

Interactive Discussion

Figure 4. Annual cycle of mean discharge after smoothing (left) and annual cycle of standard deviation after smoothing (right).
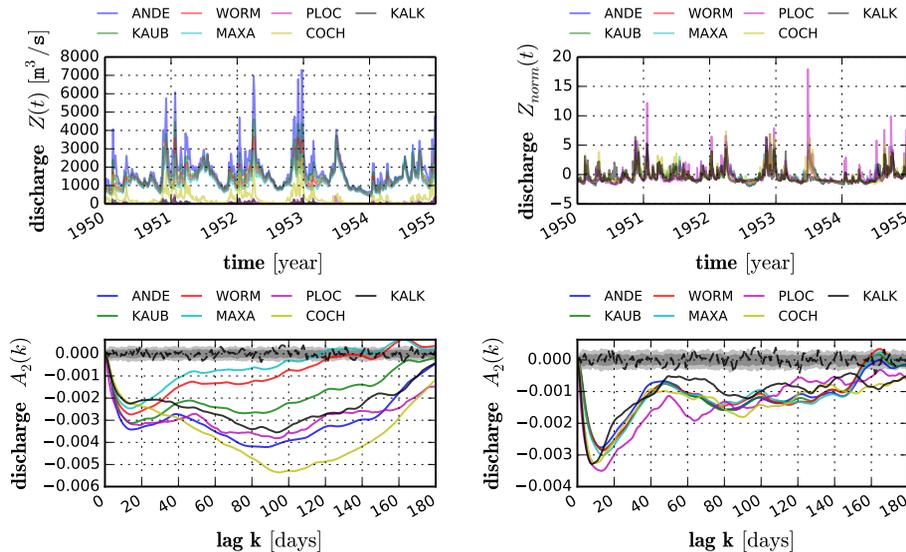
Figure 5. Discharge time series between 1950 and 1955 before applying normalization (upper left) and after applying normalization (upper right). The variation of asymmetry2 function calculated for entire time series before applying normalization (bottom left) and after applying normalization (bottom right) with 90 % confidence intervals (grey) calculated for 100 realizations of Gaussian process (dashed line is $A_2(k)$ calculated for one of the realization of Gaussian process).
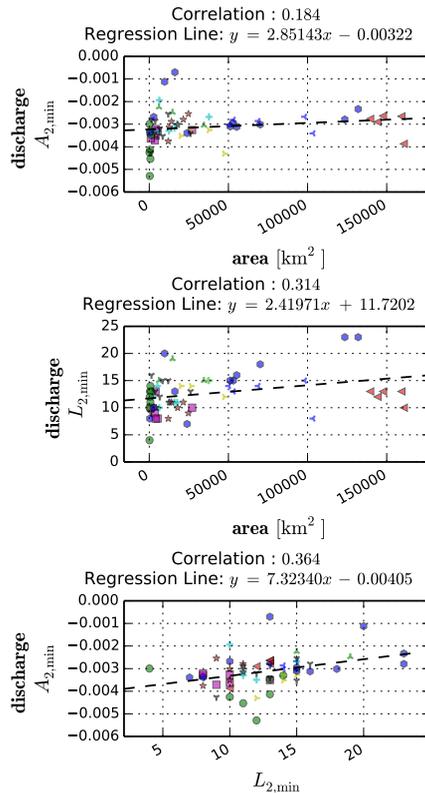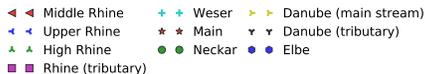
Figure 6. Relation between Asymmetry and catchment characteristics: minimum of asymmetry2 of discharge and catchment area (top), lag at minimum of asymmetry2 of discharge and catchment area (middle), minimum of asymmetry2 of discharge and lag at minimum of asymmetry2 of discharge (bottom).

Title Page

Abstract | Introduction

Conclusions | References

Tables | Figures

|◄ | ►|

◄ | ►

Back | Close

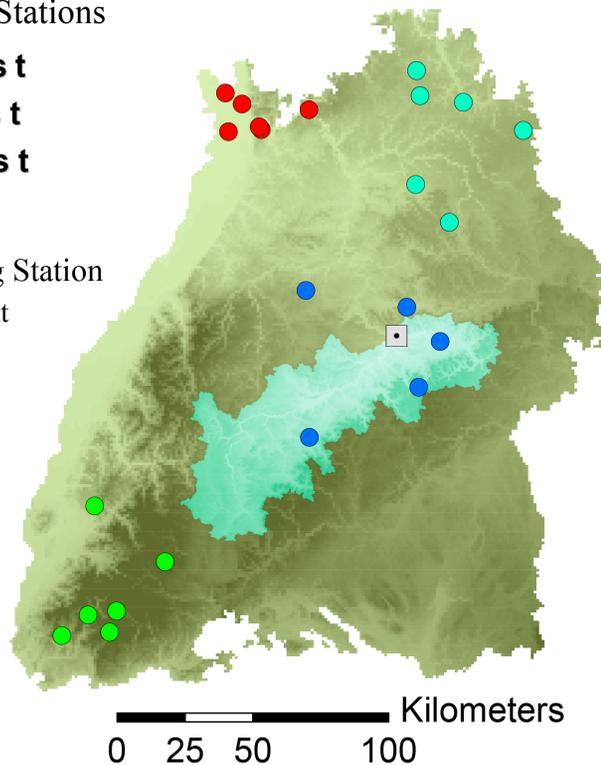Full Screen / Esc

Printer-friendly Version

Interactive Discussion
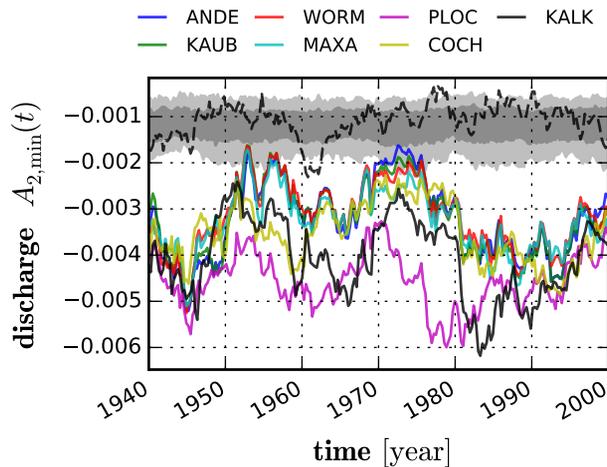
Figure 7. Temporal change of minimum of asymmetry2 for 7 discharge records and confidence intervals calculated from the Gaussian process (90 % confidence interval with grey color and 60 % confidence interval with dark grey color) and one of its realizations (dashed line).

Figure 8. Moving average and standard deviation of the 7 daily discharge records for the window size $w = 3000$.

Title Page

Abstract | Introduction

Conclusions | References

Tables | Figures

|◄ | ►|

◄ | ►

Back | Close

Full Screen / Esc

Printer-friendly Version

Interactive Discussion
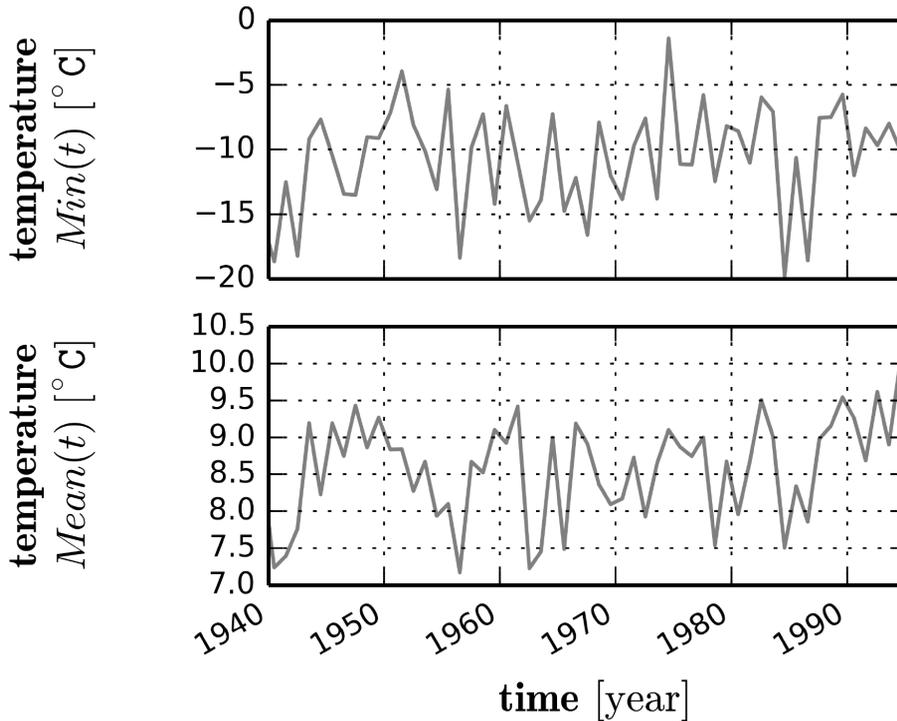
Figure 9. Annual minimum and mean of aggregated daily temperature in the Baden-Württemberg state of Germany.

Title Page

Abstract   Introduction

Conclusions   References

Tables   Figures

◄◄   ►►

◄   ►

Back   Close

Full Screen / Esc

Printer-friendly Version

Interactive Discussion
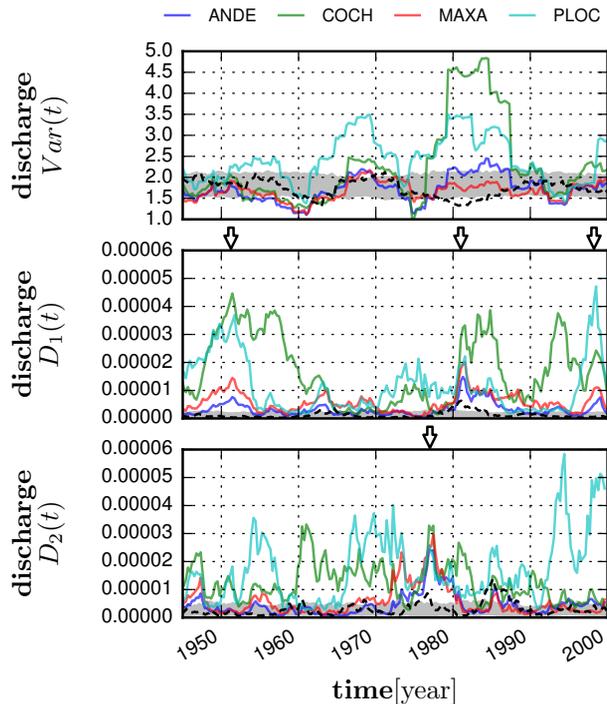
Figure 10. Copula distances of discharge time series in moving time window: moving variance (top), distance type1 (middle) and distance type2 (bottom) with 80 % confidence interval of Gaussian process and one of its realization (dashed line).

Title Page

Abstract | Introduction

Conclusions | References

Tables | Figures

|◄ | ►|

◄ | ►

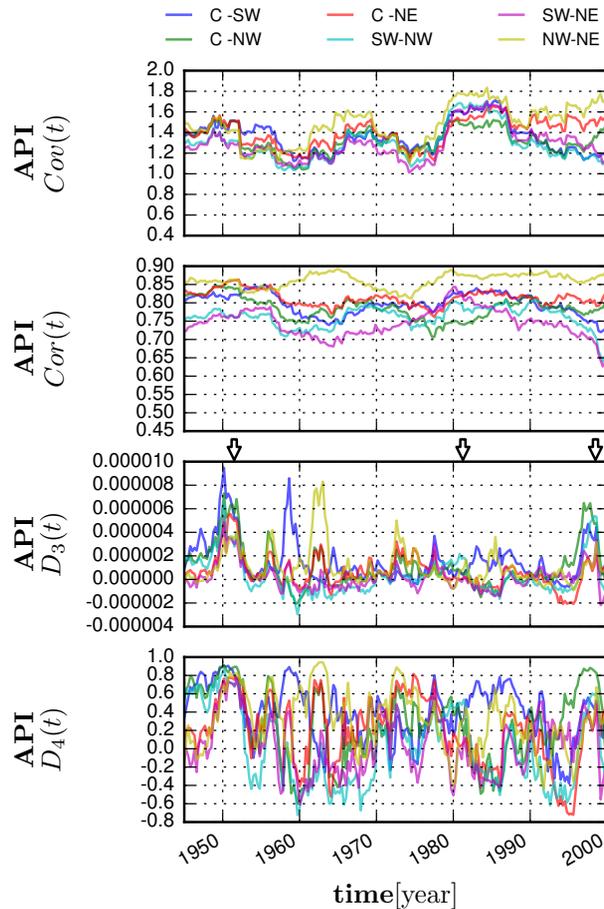Back | Close

Full Screen / Esc

Printer-friendly Version

Interactive Discussion
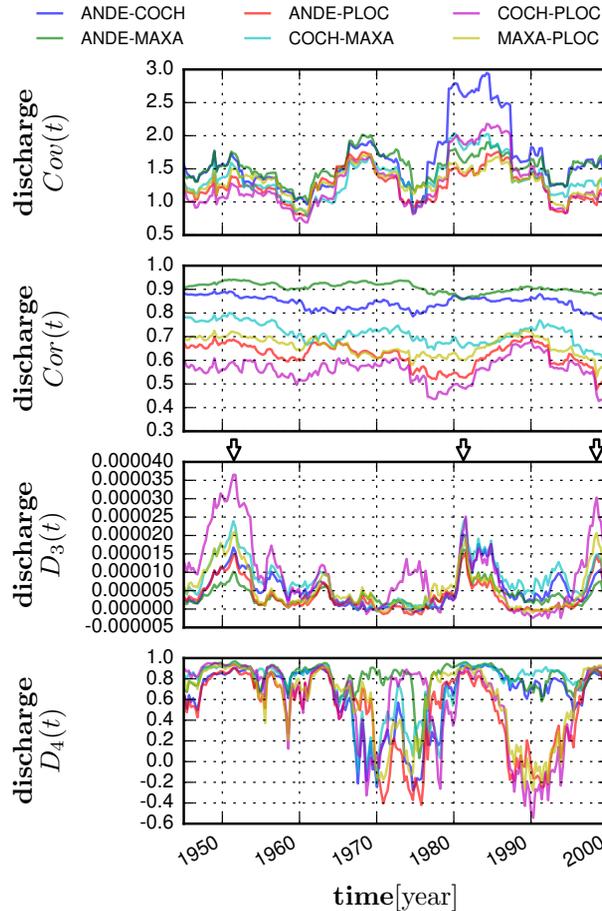
Figure 11. Copula distances of discharge time series in moving time window: moving covariance (top), moving correlation (second), distance type3 (third) and distance type4 (bottom).

Title Page

Abstract | Introduction

Conclusions | References

Tables | Figures

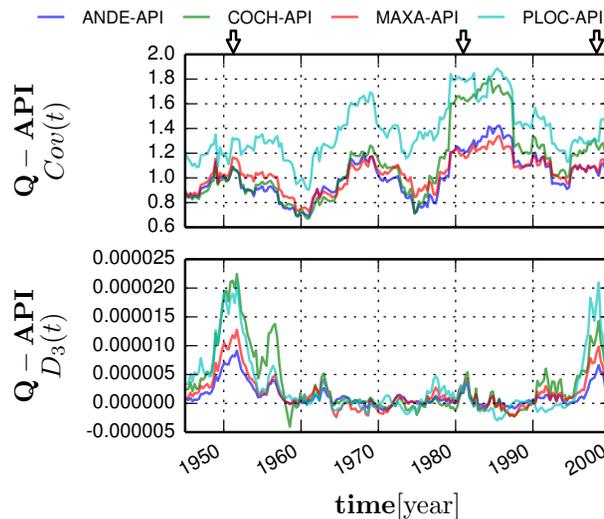|◄ | ►|

◄ | ►

Back | Close

Full Screen / Esc

Printer-friendly Version

Interactive Discussion

Figure 12. Locations of the precipitation gauge stations within the Baden-Württemberg (Germany) indicated by coloured circles. Upper Neckar catchment is drawn with green area and the location of gauging station is drawn with a square.
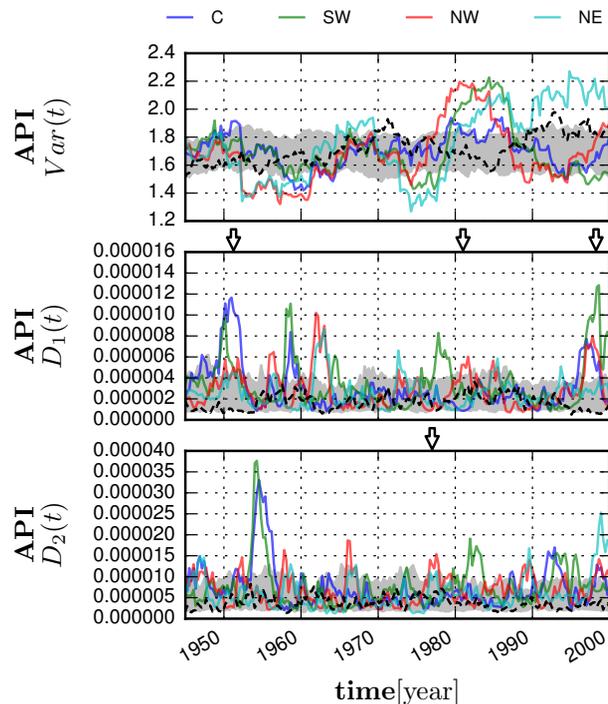
Figure 13. Copula distances of API time series in moving time window: moving variance (top), copula distance type1 (middle) and copula distance type2 (bottom) where "C" denotes central, "SW" denotes southwest, "NW" denotes northwest and "NE" denotes northeast part of Baden-Württemberg State of Germany respectively with 80 % confidence interval of Gaussian process and one of its realization (dashed line).

Figure 14. Copula distances of API time series in moving time window: moving covariance (top), moving correlation (second), distance type3 (third) and distance type4 (bottom).

Title Page

Abstract | Introduction

Conclusions | References

Tables | Figures

|◄ | ►|

◄ | ►

Back | Close

Full Screen / Esc

Printer-friendly Version

Interactive Discussion

Figure 15. Copula distance type3 (top) and type4 (bottom) between 4 discharge and 1 API time series which is aggregated for all the daily precipitations depicted in Fig. 12.
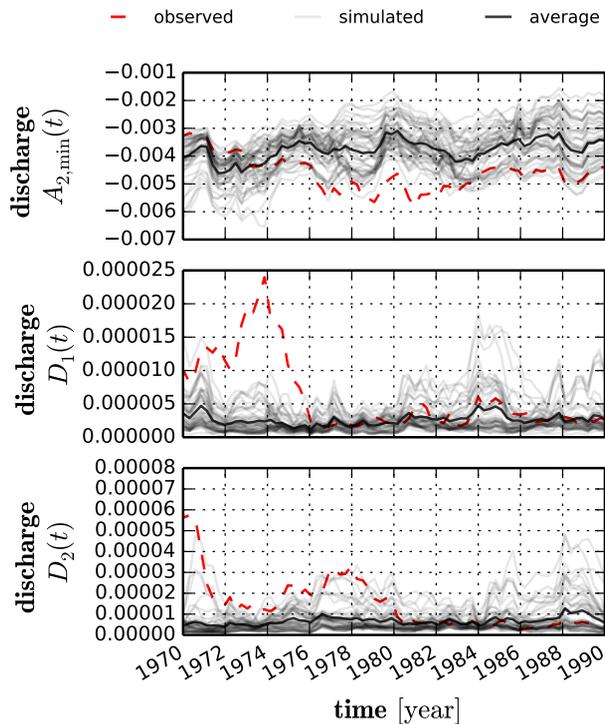
Figure 16. Copula asymmetry and copula distances for 30 simulated and one observed discharge time series at Plochingen between 1965 and 2000: minimum of asymmetry2 for the time lag $k = 2$ [days] (top), copula distance type1 (middle), copula distance type2 (bottom).